Multitemperature Resonance-Diffraction and Structural Study of the Mixed-Valence Complex [Fe$_3$O(OOCC(CH$_3$)$_3$)$_6$(C$_5$H$_5$N)$_3$]

Guang Wu, Yuegang Zhang, Lynn Ribaud, and Philip Coppens*

Chemistry Department, State University of New York at Buffalo, Buffalo, New York 14260-3000

Claire Wilson, Bo B. Iversen, and Finn Krebs Larsen

Department of Chemistry, University of Århus, DK-8000 Århus C, Denmark

Received May 15, 1998

The Fe−O and Fe−N bond lengths at two iron sites of the mixed-valence complex [Fe$_3$O(OOCC(CH$_3$)$_3$)$_6$-(C$_5$H$_5$N)$_3$] show a pronounced temperature dependence; the bonds from two of the Fe atoms to the central oxygen atoms vary by more than 0.10 Å on cooling to 10 K whereas the bond from the third iron atom is essentially invariant. The variation is such that the longest Fe−O bonds at ambient temperature are the shorter ones at 10 K, with the crossover occurring at about 90 K. The bonds to the axial pyridine ligand show the opposite dependence. The variation is attributed to an equilibrium between different configurations, which interconvert through vibronic coupling, a process that involves electron transfer between the metal atoms. The position of the absorption edge for each of the iron atoms has been determined by resonance-diffraction experiments at the Fe K edge, performed at four different temperatures. At each temperature, the order of the absorption edges corresponds to that of the experimentally determined bond lengths. The crossover near 90 K is confirmed by the resonance experiments. The absorption-edge positions are related to the formal oxidation state by calibration with reference complexes of known oxidation state. The experiments demonstrate the close relation between the changes in coordination geometry and the oxidation states of the iron atoms.

Introduction

One of the most interesting chemical applications of synchrotron radiation is based on the easy tunability of the light emitted by the synchrotron source. Because of resonance scattering that occurs near an absorption edge, the tunability allows differentiation between different oxidation states of an atom in a crystal, and it does so in a site-specific manner.[1] The method is based on the variation of the scattering power of an atom in the vicinity of an absorption edge and the dependence of the edge position on the electron binding energy, which is related to the oxidation state of the atom. Because diffraction is site-specific, it offers the capability to distinguish between oxidation states of different atoms of the same element in a crystal and is thus ideally suited for analysis of mixed-valence crystals.

In mixed-valence transition-metal complexes, bond lengths as determined by regular diffraction methods often show a pronounced temperature dependence. In most cases studied, the variation is not due to changing electron delocalization but a result of an equilibrium between different configurations, which, through vibronic coupling, are interconvertible, a process that involves electron transfer between the metal atoms. We have previously studied a series of mixed-valence μ^2-dioxo dimanganese complexes[2,3] and report here a multitemperature study on a trinuclear mixed-valence Fe complex.

When the metal atoms in a mixed-valence complex are symmetrically substituted, the configurations are identical except

for their orientation in the crystal. Energy differences between the configurations result from the packing forces acting in the crystal.

We describe here the results of multitemperature structural and resonance-diffraction studies of the trinuclear complex [Fe$_3$O(OOCC(CH$_3$)$_3$)$_6$(C$_5$H$_5$N)$_3$], for which a room-temperature structure has been reported by Cannon and co-workers.[4,5] Previous studies indicate that valence detrapping occurs over a 200 K range, as IR bandwidth measurements show a linear dependence of the logarithm of the electron-transfer rate constant with inverse temperature.[4] On the other hand, very recent Mössbauer studies have been interpreted as indicating a phase transition in the 95−101 K temperature range.[5]

The valence detrapping on temperature increase has been described as an order−disorder transition, which in many cases is accompanied by an orientational disordering of solvent molecules, which assists the intramolecular charge transfer by its change in the molecular environment.[6] However, the valence-trapped-to-valence-detrapped transitions are not limited to crystals containing solvent molecules or complexes with

(1) Coppens, P. *Synchrotron Radiation Crystallography*; Academic Press Limited: London, 1992.

(2) Coppens, P.; Bolotovsky, R.; Kezerashvili, V.; Darovsky, A.; Gao, Y. *Trans. Am. Cryst. Assoc., Proc. Symp. "Structural Tools in Organometallic and Coordination Chemistry"*, Montréal, Quebec, July 23−28, 1995; ACA: Buffalo, 1997; Vol. 31, pp 11−22.

(3) Gao, Y.; Frost-Jensen, A.; Pressprich, M. R.; Coppens, P. *J. Am. Chem. Soc.* **1992**, *114*, 9214−9215.

(4) Wu, R.; Arap Koske, S. K.; White, R. P.; Anson, C. E.; Jayasooriya, U. A.; Cannon, R. D. *J. Chem. Soc., Chem. Commun.* **1994**, 1657.

(5) Wu, R.; Pyoraz, M.; Sowrey, F. E.; Anson, C. E.; Wocadlo, S.; Powell, A. K.; Jayasooriya, U. A.; Cannon, R. D.; Nakamoto, T.; Katada, M.; Sano, H. *Inorg. Chem.* **1998**, *37*, 1913−1921.

(6) Wu, C.-C.; Hunt, S. H.; Gantzel, P. K.; Gütlich, P.; Hendrickson, D. N. *Inorg. Chem.* **1997**, *36*, 4717−4733.

easily disordered substituents such as CH$_3$. An example is [Fe$_3$O(OOCCH$_2$CN)$_6$(H$_2$O)$_3$].[7] In crystals of this complex, the phase transition occurs abruptly at 128.2 K, as measured by Mössbauer spectroscopy and heat-capacity measurements. The role of hydrogen bonding in establishing the electron-transfer equilibrium has also been emphasized.[8]

Once valence detrapping occurs, different configurations with unequal metal−ligand bond lengths are superimposed. Thus, mean-square displacement ellipsoids of the metal atoms will be elongated along the directions in which bond length variations occur. At very low temperatures, the lowest energy configuration dominates, and the disorder inherent in the electron transfer may no longer be observable. The rate of the intramolecular electron transfer and the relative energy of the different configurations are strongly affected by the solid-state environment of the mixed-valence complex.[6,8,9]

Our initial structural and resonance-diffraction studies were carried out at 150 K. Subsequently, the structure was analyzed at eight different temperatures from 10 to 295 K. The three bonds from the iron atoms to the central oxygen atom differ in length at room temperature. Two of the three bonds have values intermediate between those typical for Fe(II) and Fe(III) atoms. They are strongly temperature-dependent and show a crossover at about 90 K. This unusual behavior prompted our multitemperature resonance-diffraction study of the Fe oxidation state.

Resonance Scattering Technique. When the energy of the photons incident on a sample is close to one of the ionization energies of an atom in that sample, variations of the atomic scattering power occur. The resonance, or "anomalous" scattering affects both the real and the imaginary components of the atomic scattering factor in a narrow energy range straddling the absorption edge and is, in the isotropic limit, expressed as

$$f(S,E) = f^0(S) + f'(E) + if'(E)$$

in which f is the atomic scattering factor, E is the energy of the incident photons, and $S = \sin\theta/\lambda$ is the magnitude of the scattering vector.

The variation in the atomic scattering factor can be used to create contrast between atoms that are close in the periodic table [and therefore have very similar scattering amplitudes $f^0(S)$]. However, it can also be exploited to differentiate between atoms of the same element in difference valence states, because the ionization energies and thus the position of the edge depend on the oxidation state of the atom. Thus, the resonance occurs at different X-ray energies for atoms in different oxidation states.

In our application of the method, diffraction data are collected at a number of different wavelengths, at or near an absorption edge, on a crystal of which the structure has been determined previously. Refinement of f' and f'' of the resonating atoms at different wavelengths gives the minimum of the f' vs energy curves, which is identified with the edge position, and thus the magnitude of the chemical shift relative to that of an atom of known oxidation state.

Experimental Section

Preparation of [Fe$_3$O(OOCC(CH$_3$)$_3$)$_6$(C$_5$H$_5$N)$_3$]. The material used for all experiments at 150 K was synthesized in the manner described by Wu et al.[5] The product was recrystallized from pyridine (0.6 mL).

Table 1. Crystal Data and Structure Refinement at 150 K

empirical formula	C$_{45}$H$_{69}$Fe$_3$N$_3$O$_{13}$
formula weight	1027.58
temperature	150 K
wavelength	0.710 73 Å
crystal system	monoclinic
space group	$P2_1$
unit cell dimensions	$a = 11.651(1)$ Å, $b = 19.883(1)$ Å, $c = 11.966(1)$ Å, $\alpha = 90°$, $\beta = 106.835(4)°$, $\gamma = 90°$
volume, Z	2653.2(3) Å^3, 2
density (calculated)	1.286 Mg/m^3
absorption coefficient	0.868 mm^{-1}
F(000)	1084
crystal size	0.2 × 0.1 × 0.1 mm
no. images	45
total oscillation	0−360°
oscillation/image and overlap	10°, 2°
total no. reflections	28 058
no. unique reflections[a]	6670
θ range for data collection	2.97−23.68°
limiting indices	$0 \leq h \leq 13$, $-22 \leq k \leq 22$, $-13 \leq l \leq 12$
refinement method	full-matrix least-squares on F^2
data/restraints/parameters	6670/1/595
goodness-of-fit on F^2	1.350
R	0.0388
w$R2^b$	0.0977
absolute structure parameter	−0.01(2)
residual $\Delta\rho$ (e/Å^3)	0.42

[a] $[F^2 > 3\sigma(F^2)]$ and the Friedel pair treated as unequal. [b] $w = [\sigma(F_o^2) + 0.03(F_o^2 + 2F_c^2)/3]^{-1}$.

To avoid oxidation, the recrystallization was performed in a nitrogen atmosphere. The shiny black crystals formed were dried on filter paper for X-ray analysis. Additional specimens were provided by Dr. Palii of the Moldovan Academy of Sciences.

Structure Determination. An almost black, dark red; 0.2 × 0.1 × 0.1 mm^3 crystal was used for an analysis of the structure at 150 K. X-ray diffraction data were collected with Mo Kα radiation ($\lambda = 0.710$ 73 Å) on a MAC Science DIP-2020 imaging plate diffractometer. The crystal was cooled to 150 K by an Oxford Cryosystem Cryostream gas cooler. The DENZO program[10] was used for indexing and integration of the reflections. Cell parameters were fitted using all measured reflections; reflection intensities from different images were scaled and merged using the SCALEPACK program.[10] Data collection parameters and crystallographic information are given in Table 1. Including equivalent reflections, all reflections were observed at least twice. In the merging, the reflections whose intensities deviate from ⟨I⟩ by more than $3\sigma(I)$ were rejected. Friedel related reflections were scaled separately and not merged (space group $P2_1$). As the transmission varied little from 0.90 to 0.94 ($\mu = 0.868$ cm^{-1}), no absorption correction was applied. The SHELXTL program was used for structure determination and refinement.[11] The structure was solved by Patterson methods. H atoms were placed at calculated positions at 0.930 and 0.960 Å for CH and CH$_3$ groups, respectively. An absolute configuration test by a refinement on the inverted structure showed an obvious structural preference, giving R factors of 0.039 and 0.049 for the two enantiomorphs, respectively. The positional and thermal parameters are given in the Supporting Information, and an ORTEP plot of the complex is shown in Figure 1.

An investigation of the temperature dependence of the structure was carried out with X-ray diffraction data collected at eight different temperatures. A Bruker Smart CCD area detector diffractometer was used for data collection with Mo Kα X-rays at six temperatures (298, 200, 135, 118, 100, and 85 K; Oxford Cryosystem Cryostream gas

(7) Nakamoto, T.; Hanaya, M.; Katada, M.; Endo, K.; Kitawaga, S.; Sano, H. *Inorg. Chem.* **1997**, *36*, 4347−4359.

(8) Sato, T.; Ambe, F.; Endo, K.; Katada, M.; Maeda, H.; Nakamoto, T.; Sano, H. *J. Am. Chem. Soc.* **1996**, *118*, 3450−3458.

(9) Jang, H. G.; Geib, S. J.; Kaneko, Y.; Nakano, M.; Sorai, M.; Rheingold, A. L.; Montez, B.; Hendrickson, D. N. *Inorg. Chem.* **1989**, *111*, 173−186.

(10) Otwinowski, Z. Oscillation Data Reduction Program. In *Data Collection and Processing*, Proceedings of the CCP$_4$ Study Weekend, Jan 29−30, 1993; Sawyer, L., Isaacs, N., Bailey, S., Comp.; SERC Daresbury Laboratory: Warrington, England, 1993; pp 56−62.

(11) *SHELXTL*, version 5; Siemens Industrial Automation, Inc.; Madison, WI 1994.
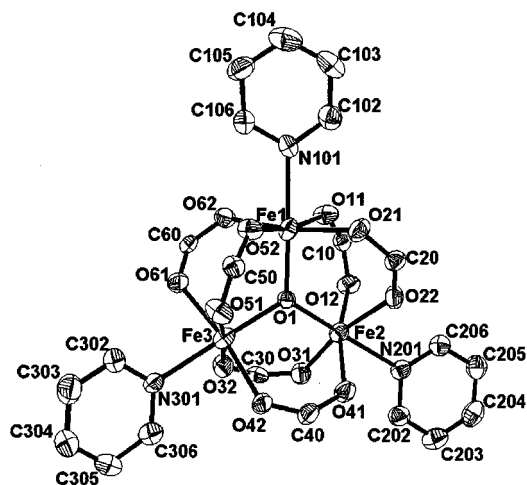
Figure 1. ORTEP plot of the structure of [Fe₃O(OOCC(CH₃)₃)₆(C₅-H₅N)₃] at 150 K. Ellipsoids are 50% probability surfaces. H atoms and butyl groups are omitted.

Table 2. Positions of the Fe Absorption Edges for a Number of Reference Compounds, the Title Compound, and the Fully Oxidized Derivative of the Title Compound

compound	formal oxidation state	absorption edge (eV)
Fe	0	7113
$FeCl_2$	II	7121
$FeNH_4(SO_4)_2$	III	7126
$Fe(NO_3)_3$	III	7127
$Fe(NO_3)_3$	III	7128
[Fe₃O(OOCC(CH₃)₃)₃)₆(C₅H₅N)₃]		7125
[Fe₃O(OOCC(CH₃)₃)₃)₆(C₅H₅N)₃]ClO₄	III	7127

cooler; crystal positioned at less than 5 mm from the tip of the nozzle). Ag Kα data were collected at 60 and 10 K on a 512 Huber four-circle diffractometer equipped with a CT211 Displex closed-cycle He cryostat. The cryogenic instrumentation was calibrated against known phase transitions of TbVO₄ (33 K) and KDP (121.6 K). The Displex temperatures are correct within 2°, and the uncertainty for the gas flow system does not exceed 5°. The full multitemperature structural study will be reported elsewhere.[12]

Resonance Scattering and Absorption Measurements. Resonance scattering and absorption measurements were carried out at the SUNY X3 beamline at the National Synchrotron Light Source. The beam energy was calibrated by measuring the K absorption edge of an Fe foil. A double-crystal Si(111) fixed-exit monochromator was used for monochromatization. To maximize the energy resolution, the focusing mirror was not inserted into the optical path. Repeated measurements of the Fe edge, using an iron foil, showed the energy to be reproducible within ±0.4 eV prior to the 150 K measurements. For subsequent energy calibration at lower temperatures, a thinner foil was used, which allows a sharper definition of the Fe absorption edge. With this foil, the energy reproducibility was found to be ±0.2 eV.

The positions of the absorption edges of a number of reference compounds, the title compound, and the fully oxidized derivative of the title compound with a ClO₄⁻ counterion are summarized in Table 2. The edge position is defined as the position of the inflection point that occurs about halfway up the edge. As the absorption measurement averages over all the absorbing atoms in the crystal, the value for [Fe₃O-(OOCC(CH₃)₃)₆(C₅H₅N)₃] represents an average over the oxidation states of the three different Fe atoms. The mixed-valence nature of the complex is evident, as the value observed is intermediate to that for the compounds with II and III oxidation states.

Diffraction data for the multiwavelength multitemperature resonance experiments were collected at 150, 100, 85, and 18 K, using a Displex cryostat for cooling. A 0.20 × 0.15 × 0.10 mm³ crystal was used for the resonance experiments at 150 K. A second crystal (0.10 × 0.07 ×
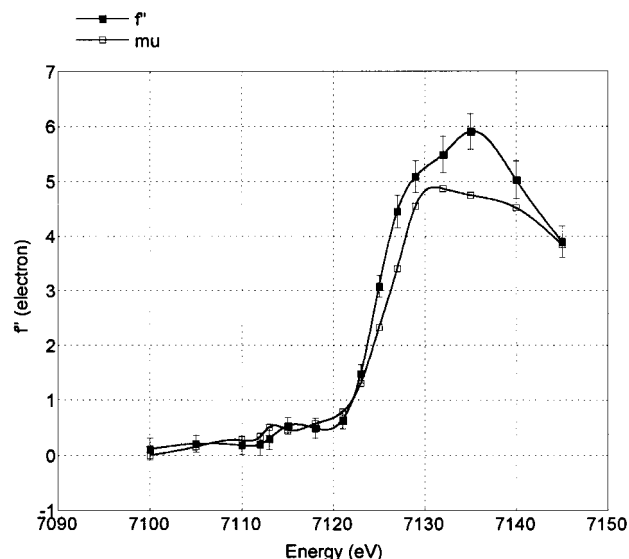
Figure 2. Average value of f'' as determined by refinement of the multiwavelength data at 150 K and the absorption coefficient μ as determined directly from the absorption measurement.

0.05 mm³) from the batch grown at the Academy of Sciences of the Republic of Moldova was used for all other measurements. At each temperature, reflections were measured at 13 energy values between 7100 and 7145 eV, spaced by 2–5 eV. At each energy at each temperature, nine images were recorded with a 25° oscillation range and a 5° overlap between consecutive images. The procedure resulted in about 100–200 unique reflections at each temperature and wavelength. As only five parameters are refined at each energy (a scale factor k, f' for each of the three iron atoms, and a common value of f''), with the other parameters being fixed at the known values at each temperature, this corresponds to a large redundancy in observations over variables.

Reflections were integrated with the program DENZO, as described above. Numerical absorption corrections were made with the program IP-ABSORB.[13] For each temperature and energy, scaling between plates was based on strong reflections; any pairs of reflections with $I < 2\sigma(I)$ were eliminated in the final calculation of the scale factors. For the refinement, only reflections measured more than once for which $(I_i - I_{ave})/I_{ave} < 5\%$ and $(I_i - I_{ave})/\sigma(I) < 2.0$ were accepted.

The weighting scheme and software used were the same as that of the structure determination. In previous work on centrosymmetric structures, we have ignored the change in f''. However, for the acentric structure analyzed here, the variation of f'' should be included in the refinement. As large correlations occurred between f'' values of the different Fe atoms, only one average value could be introduced in the final refinements. The resulting value of f'' is directly comparable with the results of the absorption measurements. The results at 150 K, shown in Figure 2, indicate the agreement to be satisfactory, thus providing support for the methods used.

Final f' vs energy curves at all four temperatures are shown in Figure 3, and the values of the f' minima are listed in Table 3.

Discussion

Temperature Dependence of the Molecular Geometry. The ORTEP drawing of the structure at 150 K (Figure 1) shows a pseudo 3-fold axis, with each of the three Fe ions being coordinated to a pyridine molecule, two bidentate pivalate ions, and the bridging O atom. The three Fe-centered octahedra thus share a corner at the central oxygen atom. Because the complex is at least partly valence-trapped at 150 K, the 3-fold symmetry is broken.

(12) Wilson, C.; Iversen, B.; Palii, S.; Larsen, F. K., to be published.

(13) De Titta, G. T. *J. Appl. Crystallogr.* **1985**, *18*, 75–79. Bolotovsky, R. Thesis, State University of New York, Buffalo, 1996.
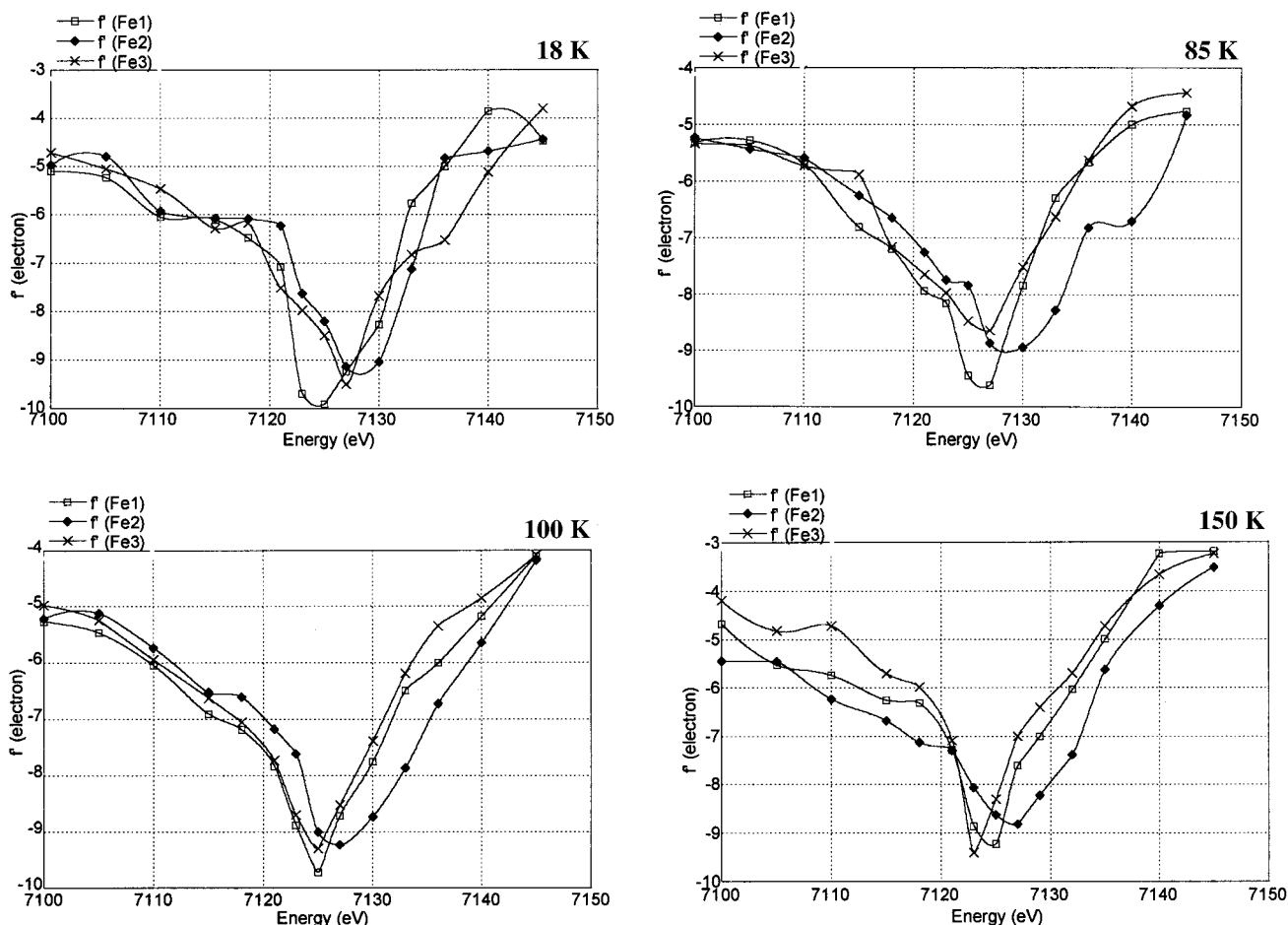
Figure 3. Anomalous scattering factor f' of Fe ions near the K edge as determined from refinement of diffraction data at different energies. Top row: 18 K, 85 K. Bottom row: 100 K, 150 K.

Table 3. Energy of f'(min) at Different Temperatures As Determined by the Resonance-Diffraction Experiment[a]

	18 K	85 K	100 K	150 K
Fe(1)	7124.1	7126.2	7124.8	7124.7
Fe(2)	7128.4	7128.3	7127.0	7126.3
Fe(3)	7127.1	7126.0	7124.9	7123.1

[a] Relative errors are estimated as ± 0.3 eV.

The temperature dependence of the bond lengths from the iron atoms to the central oxygen atom is illustrated in Figure 4a. The Fe(2)−O bond length is almost independent of the temperature and has a value typical for an Fe(III)−O bond. This is in accordance with the observation by Wu et al.[4,5] that the Fe(2) atom is not involved in electron transfer upon temperature change. The same invariance of the oxidation state of one of the three Fe atoms has been observed in [Fe$_3$O(OOCCH$_2$Cl)$_6$-(H$_2$O)$_3$][8] and other complexes.

In contrast, the other Fe−O bond lengths are strongly temperature-dependent. Although the Fe(3)−O distance is the longest at room temperature [1.951(3) Å], after an increase to about 1.989(3) Å near 135 K, it steadily decreases to reach 1.862(6) Å at 10 K. At that temperature, this distance is almost equal to that of Fe(2)−O. The Fe(1)−O length has the intermediate value of 1.914(3) Å at room temperature. As the crystal cools, this bond length decreases to a minimum of 1.897 Å near 135 K and then increases to a maximum value of 2.040(6) Å at 10 K, with the crossover taking place at about 90 K.

The bond lengths determined at 150 K, with a specimen synthesized in Buffalo, are marked by the large crosses in Figure 4a. Although they are in general agreement, they do not quite fall on the curves through the other points. Because the crystals came from different sources, this suggests that the temperature dependence of the bond lengths may be somewhat sample-dependent. Likewise, the variation of the crystal mosaicity is different for the two crystals examined, as discussed further below.

Examination of Figure 4a shows that the bond-length curves for Fe(1) and Fe(3) are quite symmetrical around a value of 1.94 Å, with an increase in one length being matched by a decrease in the second. Assuming a linear dependence of the bond length on average oxidation state, this implies that the sum of the oxidation states of Fe(1) and Fe(3) is constant. Because the Fe(2)−O distance is practically temperature-independent, the sum of the oxidation states is then invariant, a reasonable result, given the requirement of charge neutrality of the crystal. Thus, the bond-length analysis confirms that the electron transfer occurs almost exclusively between Fe(1) and Fe(3).

In agreement with this result, the ORTEP diagrams at higher temperatures show that the displacement ellipsoids for Fe(1) and Fe(3) are elongated in the direction of the central oxygen atom. This is not the case for the oxidation-state-invariant Fe(2) atom (Figure 1). A similar observation was made earlier in the room-temperature study.[5]

The Fe−O(pivalate) bonds show a temperature dependence that is similar to but smaller than that of the Fe−O(1) bonds (Figure 4b). The dependence of the distances of the Fe atoms to the nitrogen atom of the coordinated pyridine molecules is

a

b

c
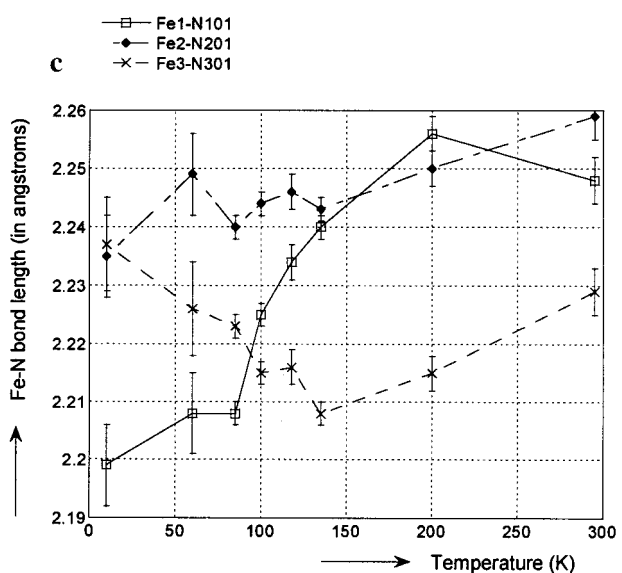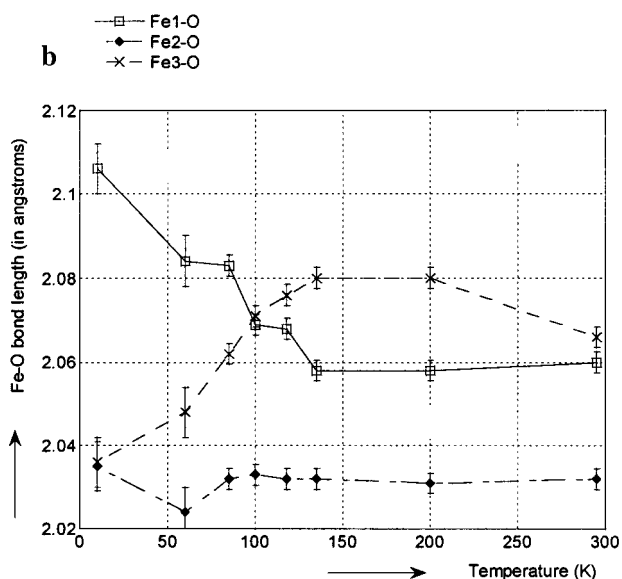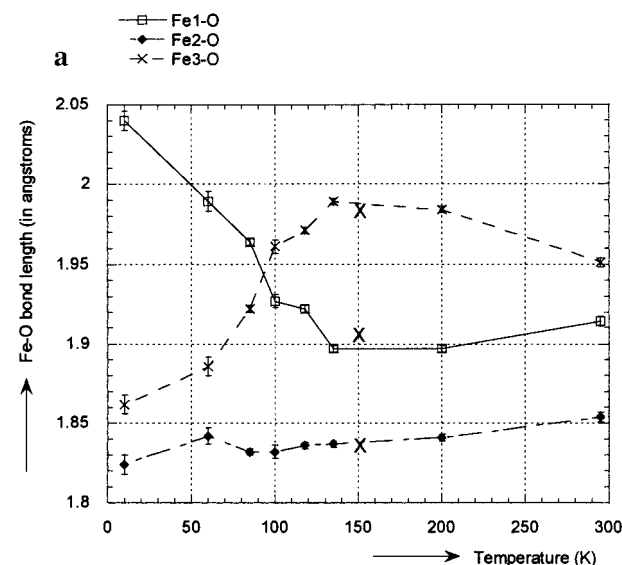
Figure 4. Bond lengths vs temperature. (a) Fe−O(1) the large crosses indicate the values of the 150 K structure determination on a different crystal. (b) Fe−O (pivalate), each curve represents an average over four chemically equivalent Fe−O bonds. (c) Fe−N (pyridine).
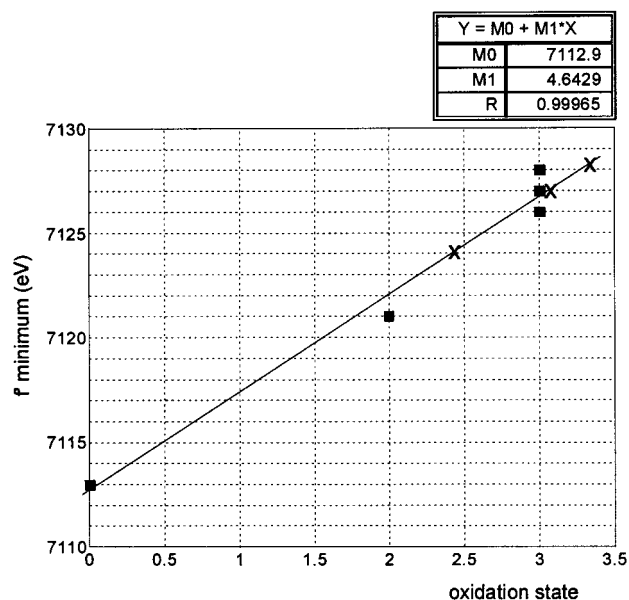
Figure 5. Edge positions, indicated by squares, of a number of Fe compounds vs formal oxidation state. The line represents the best linear fit through the points. The crosses, placed on the calibration line, indicate the experimental values for the title complex at 18 K. The compounds and numerical values are listed in Table 2.

shown in Figure 4c. Although the absolute values of the distance changes are less pronounced, the crossover of the Fe(1) and Fe(3) distances near 90 K is evident here also. However as noticed previously,[5] the order of the Fe−N distances is the reverse of that of the Fe−O(1) bond lengths. This feature is retained at all temperatures, with the possible exception of 200 K, at which Fe(1)−N and Fe(2)−N appear practically equal. The change of shape of the molecular envelope because of the Fe−O(1) bond variation is apparently compensated for at least in part by the changes in the Fe−N distances.

Cooling induces a reversible increase of the mosaicity of the crystals, starting around 100 K. The change is attributed to strain induced by the varying shape of the molecular envelope. The increase is sample-dependent. It was found to be much larger in the crystal used for the initial 150 K measurements than for those used in the diffraction experiments at the other temperatures.

Resonance Results. A calibration curve for Fe at different oxidation states is given in Figure 5. It shows the relation between oxidation state and the position of the absorption edge to be very close to linear, as observed previously for vanadium and its oxides.[14] The slope of the curve is 4.6 eV/oxidation state unit, which is close to the difference between the Fe(2) and Fe(1,3) f' minima at 18 K (Table 3). It should be noted, however, that the observed edge positions for the three complexes with oxidation states of III differ by about 1 eV. Oxidation state is a formal concept, but the ionization energy is a physical quantity, so any correlation can only be qualitative. The ionization energy as measured by the resonance experiment obviously contains more detailed information than can be inferred from the formal oxidation state.

The values of the edge position of the Fe atoms in the title compound have been derived from the positions of the minima of the curves in Figure 3 and are plotted in Figure 6. Error bars corresponding to 1 standard deviation are indicated in the figure. The results confirm the crossover in oxidation state that occurs during cooling of the samples. *At each temperature,*

(14) Wong, J.; Lytle, F. W.; Mesmer, R. P.; Maylotte, D. H. *Phys. Rev. B: Condens. Matter* **1984**, *30*, 5596−5610.
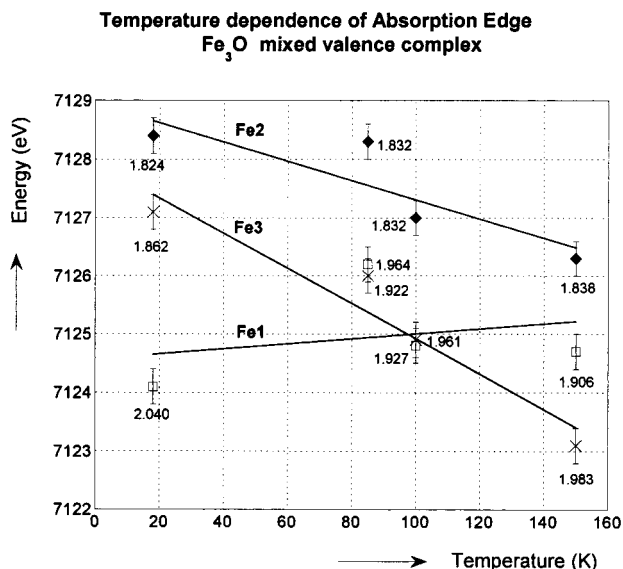
Figure 6. Position of the f' minimum of the three Fe atoms as a function of temperature. The numbers represent the Fe−O(1) bond lengths at the different temperatures. At 18 K, the bond lengths measured at 10 K are given.

the order of the minima corresponds to the order of the experimentally determined bond lengths. At 18 K, for example, the order is Fe(1) < Fe(3) < Fe(2). The observed Fe(1) and Fe(3) absorption-edge positions become equal at about 85−100 K and then interchange, with the edge for Fe(1), which is at the lowest energy at 18 K, being intermediate between Fe(2) and Fe(3) at the higher temperatures (Table 3). It is evident that the observed bond-length crossover is related to the variation of the average oxidation state of each of the sites.

Examination of Figure 6 suggests that in the separately performed experiment at 150 K the absolute energy may have been underestimated, that the sample used may have exhibited a somewhat different behavior, or that both may have occured, as indicated by the bond-length differences discussed above. Nevertheless, the observed values of the edge for Fe(2) show the smallest variation with temperature and are typical for Fe(III). Given the uncertainty in the 150 K measurements and the experimental error bars, the resonance experiments are compatible with the conclusion of invariance of the Fe(2) oxidation state, as based on the lack of temperature variation of the bond lengths involving Fe(2) (Figure 4) and with the $M^{2+} + M^{3+} \rightarrow M^{3+} + M^{2+}$ mechanism discussed by Wu et al.[5]

An increase in the width of the f' minima in Figure 3 might be expected at temperatures at which two oxidation states are superimposed, but no such broadening is observed. On the contrary, the ordered Fe(2) site seems to give a broader, rather than a narrower, minimum. The broadening could be due to transitions to empty-but-bound states at Fe(III), which may not be resolved at the experimental energy resolution. It should also be noted that the curves are averages over all possible orientations of the f' tensor. Because the coordination at the iron atoms is pseudooctahedral, the anisotropy of f' should not be pronounced. However, if f' for Fe(2) was more anisotropic than the anomalous scattering factors of the other iron atoms, the broader minimum that is observed could be explained on this basis. Analysis of such effects awaits the higher energy resolution that can be achieved at third-generation synchrotron sources. No preedge features are resolved in the current experiments.

Nature of the Equilibrium. As noted before, [Fe₃O(OOCC-(CH₃)₃)₆](C₅H₅N)₃] belongs to a class of trinuclear iron com-

plexes in which electron transfer is limited to two of the three iron atoms. Wu et al. conclude, from variable-temperature Mössbauer experiments, that a phase transition occurs over the range 96−101 K. They propose that below the phase transition there are two sets of structurally distinct molecules, both with the fully localized electronic configuration $Fe^{III}_2Fe^{II}$.[5] Such a phase transition has been reported in the case of [Fe₃O(OOC-(CH₃)₃)₆(C₅H₄ClN)₃](C₅H₄ClN)₃.[6] Our results on [Fe₃O(OOCC-(CH₃)₃)₆(C₅H₅N)₃] are not in agreement with a structural phase transition to a fully valence-trapped state near 100 K, though there is a marked decrease in the apparent thermal motion of the butyl groups on cooling. Even below the crossover at about 90 K, the two atoms with the highest oxidation state differ in coordination geometry and the position of the f' minima. However, the two Fe atoms become very close to equivalent at 10 K.

It has been noted that the observed lack of 3-fold symmetry of the molecule in solution favors a dynamic electron-hopping mechanism over a static delocalization,[4] a conclusion supported by the subsequent Mössbauer experiments.[5] According to the analysis of spectroscopic line widths, the logarithm of the rate of electron transfer is linear with temperature in the 410−480 K range and extrapolates to an essentially zero transfer rate at 10 K. However, the diffraction experiments show that the coordination geometries of Fe(1) and Fe(3) at 10 K are not exactly equal and the edge positions of the two metal atoms at 18 K are not the same. Thus, there may be static disorder remaining in the crystals at low temperature.

The electron-transfer equilibrium changes the average shape of the complex in the anisotropic crystal environment and is therefore influenced by the packing forces in the crystal. These are temperature-dependent because of the thermal contraction on cooling and possible onset of disorder when solvent molecules or easily rotating groups are present. At higher temperatures, the exchange becomes rapid, and entropy effects will favor a more equal distribution of the electrons over the two Fe sites involved in the transfer. As is evident from Figure 4, at room temperature the Fe(1) and Fe(3) sites are practically identical.

Conclusion

The agreement between the multitemperature resonance experiments and the structural results establishes a relation between the observed FeO bond lengths and the site-averaged oxidation state. It supports the validity of the resonance-diffraction technique as a probe for the electronic structure of atoms. Unlike Mössbauer spectroscopy, resonance diffraction is applicable to a wide variety of elements.

Supporting Information Available: Tables of crystal data and structure refinement, atomic and thermal parameters for 10 and 150 K structures; bond lengths and angles at 10 K; experimental values of f' and f'' standard deviations and R factors of the resonance refinement at 18, 85, 100, and 150 K (13 pages). Ordering information is given on any current masthead page.

IC980556B